

Squeezing of quantum noise

Jinyuan Wu

December 16, 2022

Abstract

Systems isolated from external disturbance still have noises arising from the uncertain nature of quantum observables, which set a limit to the precision of linear quantum optics interferometers. This report visualizes quantum noise using Wigner function, analyzes the quantum noise in Mach-Zehnder interferometer in the small phase difference limit, and demonstrates the quantum noise can be “squeezed” by changing the dark port input in an intuitive way according to the visualization.

1 Introduction

Noise usually arises from coupling with an unknown environment: when we keep our eyes only on one of the system, we need to average over the state of the environment, which corrects the equation of motion of the system with noise and dissipation [1]. However, systems isolated from the outside world still have noise: if the wave function of the system is not an eigenstate of the observable in question, any experimental setting measuring that observable has noisy results. This kind of noise is called **quantum noise**.

In systems that can be well described by harmonic oscillators, for each oscillation mode, we have two variables X and P , and $[X, P] = i$ (here and below we use Planck system of units), and the Hamiltonian is $H \simeq c_1 X^2 + c_2 P^2$ plus possible interaction perturbations. After diagonalization, we get $H \simeq \sum_{\text{modes}} \omega(a^\dagger a + 1/2)$, which may be further modified by interaction terms. The zero-point energy $1/2$ arises from the non-commutative nature of X and P . Another way to see the quantum nature of the zero-point energy is to note that at the ground state, though $\langle X \rangle = \langle P \rangle = 0$, since we have the zero-point energy, $\langle X^2 \rangle, \langle P^2 \rangle \propto \langle H \rangle / 2 \neq 0$. We therefore sometimes say that quantum noise comes from the zero point-energy. Of course, by manipulating the quantum state, the variance of *one* degree of freedom may be reduced, at the cost of larger variances on other degrees of freedom. This is called “squeezing” of the quantum noise.

This report focuses on quantum noises in linear quantum optics interferometry, which fits in the picture described above. Section 2 discusses quantitative ways to represent and characterize quantum noise. Section 3 calculates quantum noise in Mach-Zehnder interferometer. Section 4 demonstrates that when the input laser beam is strong enough, the quantum noise in the output can be attributed to the quantum noise in the dark port. Section 5 shows how to squeeze the quantum noise in the output by injecting a squeezed state into the dark port.

2 Quantum optics states and quasi-probability distribution functions

In linear quantum optics, we have [4]

$$H = \int d^3 \mathbf{r} \left(\frac{1}{2} \epsilon \mathbf{E}^2 + \frac{1}{2\mu} \mathbf{B}^2 \right) = \sum_k \omega_k \left(a_k^\dagger a_k + \frac{1}{2} \right), \quad (1)$$

where k is the label of the optical normal mode \mathbf{f}_k and

$$\mathbf{E} = \sum_k \mathcal{E}_k \mathbf{f}_k a_k e^{-i\omega_k t} + \text{h.c.}, \quad \mathcal{E}_k = \sqrt{\frac{\hbar \omega_k}{2\epsilon_0 V}}, \quad \frac{1}{V} \int d^3 \mathbf{r} \mathbf{f}_{k'}^* \cdot \frac{\boldsymbol{\epsilon}}{\epsilon_0} \cdot \mathbf{f}_k = \delta_{kk'}. \quad (2)$$

The label k is the momentum and polarization in a large box, and in an spherical optical cavity, it labels spherical harmonics. We have the standard bosonic commutation relations

$$[a_k, a_{k'}] = 0, \quad [a_k, a_{k'}^\dagger] = \delta_{kk'}. \quad (3)$$

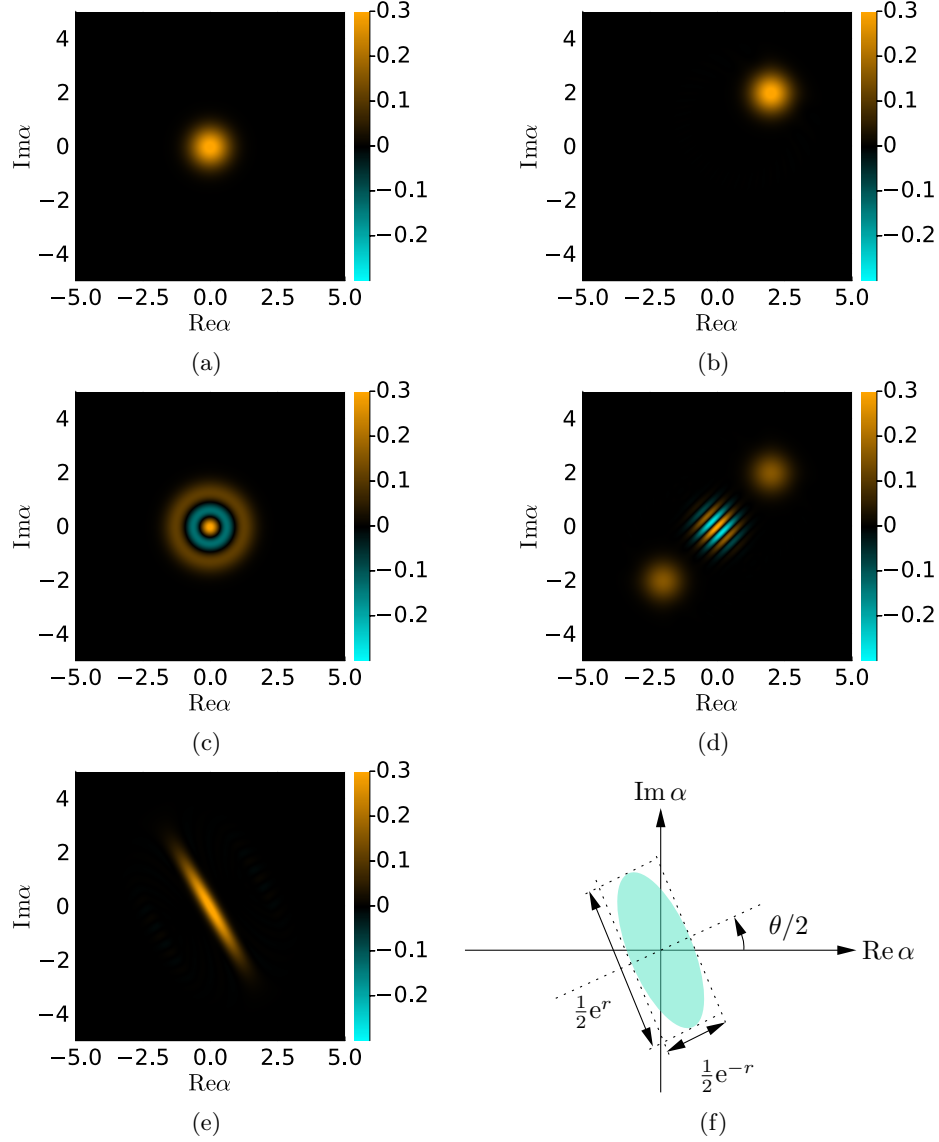


Figure 1: Wigner functions in quantum optics. Figures are plotted using `QuantumOptics.jl` [2]. (a) The Wigner function of the vacuum. Note that this is not a δ -function located at $\alpha = 0$. (b) The Wigner function of $|\alpha = 2 + 2i\rangle$. (c) The Wigner function of a double-photon state. Negative values occur. (d) The Wigner function of $(|\alpha = 2 + 2i\rangle + |\alpha = -2 - 2i\rangle)/\sqrt{2}$. (e) The Wigner function of $S(e^{i\pi/3})|0\rangle$. (f) Schematic illustration of the Wigner function of a squeezed vacuum state $S(re^{i\theta})|0\rangle$. The uncertainty relation (6) is observed. The diagram is adapted from Fig. 2.8 in [3].

To visualize a quantum state and the quantum noise in it, so-called quasi-probability distribution functions may be utilized. For one mode, if a and a^\dagger in an arbitrary operator O is ordered according to a certain convention (a before a^\dagger , or a^\dagger before a , or whenever multiplication appears, it is in the form of $(a^\dagger a + a a^\dagger)/2$), we have

$$\langle O(a, a^\dagger) \rangle = \int d^2\alpha f(\alpha, \alpha^*) O(\alpha, \alpha^*), \quad (4)$$

where $O(\alpha, \alpha^*)$ is the polynomial form of O in terms of a, a^\dagger with the correct ordering applied to dummy variables α and α^* . Here α can be roughly conceived as the “value” of a . We say $f(\alpha, \alpha^*)$ is a quasi-probability distribution function. Note that this definition even extends to the case when we are in a mixed state instead of a pure state, i.e. it is a unified treatment of both quantum noise and thermal noise.

To plot the function as a 2D heatmap, it is often more convenient to change the coordinates into $\text{Re } \alpha$ and $\text{Im } \alpha$. Note that we have

$$[\text{Re } a, \text{Im } a] = \frac{1}{4i} [a + a^\dagger, a - a^\dagger] = \frac{i}{2}, \quad (5)$$

and according to the uncertainty principle, we have

$$\Delta(\text{Re } a) \cdot \Delta(\text{Im } a) \geq \frac{1}{4}. \quad (6)$$

Another frequent convention is to define

$$a = \frac{1}{\sqrt{2}}(X + iP), \quad a^\dagger = \frac{1}{\sqrt{2}}(X - iP), \quad (7)$$

and we find $[X, P] = i$. Here the $\sqrt{2}$ factor is simply there to normalize the commutation relation.

The most famous quasi-probability distribution is probably the **Wigner function**, and it is the quasi-probability distribution used in this report. The Wigner function of a density matrix ρ (which is $|\psi\rangle\langle\psi|$ for a pure state) is defined as [3]

$$W(x, p) = \frac{1}{\pi\hbar} \int_{-\infty}^{\infty} \langle x - y | \rho | x + y \rangle e^{-2ipy/\hbar} dy, \quad (8)$$

and we can use (7) to define $W(\alpha, \alpha^*)$ and hence $W(\text{Re } \alpha, \text{Im } \alpha)$.

Some examples of pure state Wigner functions are given in Fig. 1. Fig. 1(a) is the Wigner function of the vacuum state: there is no photon, and the distribution of probability is focused on $\alpha = 0$. Note that it is not a δ -function, and is somehow “blurred”: this is a visualization of (6). Not all two-variable functions can be a Wigner function: they cannot have too strong “spatial resolution”. The vacuum state is a specific case of the family of **coherent states**. A coherent state labeled by the complex parameter α is defined as

$$|\alpha\rangle = D(\alpha) |0\rangle = e^{\alpha a - \alpha^* a^\dagger} |0\rangle, \quad a |\alpha\rangle = \alpha |\alpha\rangle. \quad (9)$$

In the classical limit, the electric field of a light field in $|\alpha\rangle$ is $\mathbf{E} = \alpha \mathbf{f} e^{-i\omega t} + \text{c.c.}$, where \mathbf{f} is the mode function. Fig. 1(d) is an example of a coherent state with $\alpha \neq 0$. Fig. 1(c) and (d) are Wigner functions of a Fock state (i.e. an eigenstate of $n = a^\dagger a$) and a superposition state of two coherent states. We have $\langle \mathbf{E} \rangle = 0$ for a Fock state, because $\langle n | a | n \rangle = 0$, but $\langle \mathbf{E}^2 \rangle \neq 0$. Fig. 1(d) is a prototypical “cat” state. Therefore both of them are far from classical states, and correspondingly the Wigner functions of them have negative values, which is impossible for a classical probability distribution. Fig. 1(e) is a “squeezed vacuum”. To squeeze a state with the complex parameter ξ means to apply

$$S(\xi) = e^{\frac{1}{2}(\xi^* a^2 - \xi (a^\dagger)^2)} \quad (10)$$

to that state. The schematic Wigner function of a squeezed vacuum state with parameter $\xi = r e^{i\theta}$ is illustrated in Fig. 1(f). It can be seen that with $S(\xi) |0\rangle$, we have [3]

$$\Delta \left(\cos \frac{\theta}{2} \text{Re } a + \sin \frac{\theta}{2} \text{Im } a \right) = \frac{1}{2} e^{-r}, \quad (11)$$

while

$$\Delta \left(\sin \frac{\theta}{2} \text{Re } a - \cos \frac{\theta}{2} \text{Im } a \right) = \frac{1}{2} e^r. \quad (12)$$

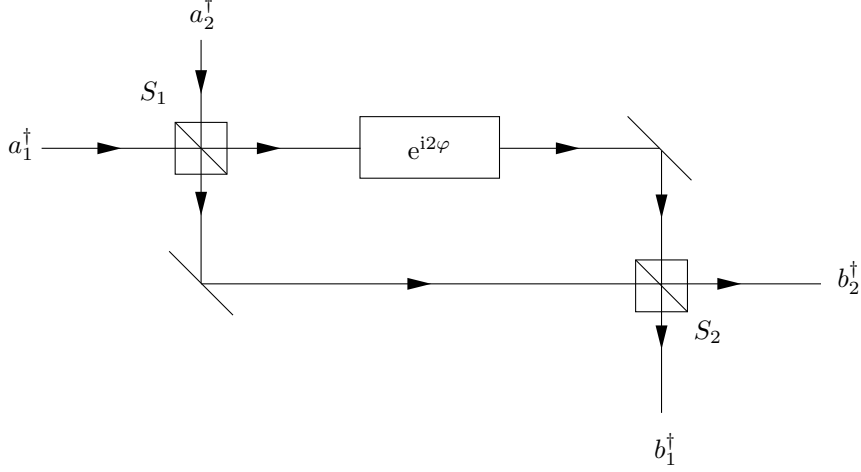


Figure 2: The schematic structure of the Mach-Zehnder interferometer

3 Quantum noise in the Mach-Zehnder interferometer

To have a concrete example of quantum noise, let us move to the **Mach-Zehnder interferometer** [5], illustrated in Fig. 2. The interferometer contains two beam splitters, two ideal mirrors, and one sample that introduces a 2φ phase shift to the light beam going through it. The two beams created by the first beam splitter gain a phase difference caused by the sample, and are then remixed together by the second beam splitter, so there is interference, and φ can be found by comparing the output signal with the injected laser beam.

We are going to work in the Heisenberg picture, because the whole system is linear and time evolution can be easily described by a linear transformation on the operators. Since this section is just to exemplify the overall idea of quantum noise, for the sake of simplicity we assume the time evolution operator of the beam splitter is

$$S_{\text{beam splitter}} = \frac{1}{\sqrt{2}} \begin{pmatrix} 1 & 1 \\ -1 & 1 \end{pmatrix}. \quad (13)$$

The time evolution operator of the whole system is therefore

$$\begin{aligned} S_{\text{total}}(\varphi) &= \frac{1}{\sqrt{2}} \begin{pmatrix} 1 & -1 \\ 1 & 1 \end{pmatrix} \cdot \begin{pmatrix} e^{i\varphi} & \\ & e^{-i\varphi} \end{pmatrix} \cdot \frac{1}{\sqrt{2}} \begin{pmatrix} 1 & 1 \\ -1 & 1 \end{pmatrix} \\ &= \begin{pmatrix} \cos \varphi & i \sin \varphi \\ -i \sin \varphi & -\cos \varphi \end{pmatrix}, \end{aligned} \quad (14)$$

and therefore¹

$$\begin{pmatrix} b_1 \\ b_2 \end{pmatrix} = \begin{pmatrix} \cos \varphi & i \sin \varphi \\ -i \sin \varphi & -\cos \varphi \end{pmatrix} \begin{pmatrix} a_1 \\ a_2 \end{pmatrix}, \quad \begin{pmatrix} b_1^\dagger \\ b_2^\dagger \end{pmatrix} = \begin{pmatrix} \cos \varphi & -i \sin \varphi \\ i \sin \varphi & -\cos \varphi \end{pmatrix} \begin{pmatrix} a_1^\dagger \\ a_2^\dagger \end{pmatrix}, \quad (15)$$

from which we find

$$\begin{pmatrix} a_1^\dagger \\ a_2^\dagger \end{pmatrix} = \begin{pmatrix} \cos \varphi & -i \sin \varphi \\ i \sin \varphi & -\cos \varphi \end{pmatrix} \begin{pmatrix} b_1^\dagger \\ b_2^\dagger \end{pmatrix}. \quad (16)$$

In actual experiment settings, usually a beam of laser is injected into input port 1, so the state at input port 1 is a coherent state. Then, the wave function is

$$\begin{aligned} |\psi\rangle &= \underbrace{e^{\alpha a_1 - \alpha^* a_1^\dagger}}_{D_{a_1}(\alpha)} |0\rangle \\ &= e^{\alpha(\cos \varphi b_1^\dagger - i \sin \varphi b_2^\dagger) - \alpha^*(\cos \varphi b_1 + i \sin \varphi b_2)} |0\rangle \\ &= D_{b_1}(\alpha \cos \varphi) D_{b_2}(-i \alpha \sin \varphi) |0\rangle. \end{aligned} \quad (17)$$

¹Note that the EOM of the annihilation operators in the Heisenberg picture has the same form with the EOM of the wave function in the Schrödinger picture.

Note that the state in a_2 subspace remains vacuum; it is a convention to call a_2 the **dark port**.

The next step is measurement. For simplicity we assume $\varphi \ll 1$, and therefore the signal in the b_2 mode is $\sim \varphi$, while the signal in the b_1 mode is $\sim \varphi^2$ (the signal in the b_1 mode should be defined as $\alpha - \alpha \cos \varphi$). So we consider the expectation of n_{b_2} , which is

$$\langle n_{b_2} \rangle = |\alpha|^2 \sin^2 \varphi. \quad (18)$$

This output comes with a quantum uncertainty, which is given by

$$\begin{aligned} \Delta n_{b_2} &= \sqrt{\langle n_{b_2}^2 \rangle - \langle n_{b_2} \rangle^2} \\ &= \sqrt{\langle b_2^\dagger (b_2^\dagger b_2 + 1) b_2 \rangle - \langle n_{b_2} \rangle^2} \\ &= \sqrt{|\alpha|^4 \sin^4 \varphi + |\alpha|^2 \sin^2 \varphi - |\alpha|^4 \sin^4 \varphi} \\ &= |\alpha| \sin \varphi. \end{aligned} \quad (19)$$

Here we have used the property of coherent states as eigenstates of the annihilation operator.

So it can be seen that the relative uncertainty of the measurement is

$$\frac{\Delta n_{b_2}}{\langle n_{b_2} \rangle} = \frac{|\alpha| \sin \varphi}{|\alpha|^2 \sin^2 \varphi} = \frac{1}{\sqrt{\langle n_{b_2} \rangle}}. \quad (20)$$

It can be seen from (19) that this standard error comes from the commutation relation $[b_2, b_2^\dagger] = 1$, which, eventually, comes from the fact that \mathbf{E} and \mathbf{A} in electromagnetism don't commute. This is therefore a quantum noise.

Of course, (20) can be systematically reduced by increasing laser intensity, so even if the quantum noise is always present, its influence can be progressively reduced. But the detecting laser beam is another source of noise. In the example of gravitational wave detection, the mirrors used will be perturbed by the momenta of the photon jet arriving at them, and since the number of photons has quantum fluctuation, so is the motion of the mirrors, and another noise is introduced to φ [6, 7]. Classically, we can successively weaken the laser beam and get an infinite sequence of measurements with shrinking disturbance of the system, the true value of the observable in question being the limit of this sequence. But we know weakened laser beam means higher relative error introduced by the quantum noise.

Thus, astonishingly, when quantum noise is present, even in principle, unboundedly improving the precision is not possible. There is a non-zero minimal noise, which is achieved when $|\alpha|$ strikes a balance between the thermal fluctuation caused by large $|\alpha|$ and quantum noise caused by small $|\alpha|$ [5].

4 The quantum noise as the fluctuation of the dark port

One thing to keep in mind is (20) is about the quantum noise of the photon number, not others. This quantity is not the only observable in b_2 mode, but it is the only thing actually measured. Thus it is possible that we reduce the quantum noise of n_{b_2} and in exchange, get a larger quantum noise of other variables, which we do not care. This is called “squeezing” the quantum noise – the term will be visualized in the following discussion. To do so, it is necessary to trace the origin of Δn_{b_2} in terms of quantum noises of a_1 and a_2 . For sake of simplicity, here we keep the input state in the a_1 mode $|\alpha\rangle$, without modifying anything, and we also exclude all cross terms between a_1 and a_2 in the wave function, so we have

$$|\psi\rangle = D_{a_1}(\alpha) f(a_2, a_2^\dagger) |0\rangle, \quad (21)$$

and squeezing Δn_{b_2} therefore reduces to squeezing the quantum noise of some operator in mode a_2 .

From (15), we have

$$n_{b_2} = b_2^\dagger b_2 = \sin^2 \varphi a_1^\dagger a_1 + \cos^2 \varphi a_2^\dagger a_2 - i \sin \varphi \cos \varphi (a_1^\dagger a_2 - a_2^\dagger a_1). \quad (22)$$

In the subspace determined by (21), all a_1 can be replaced by α in the above two equations, but before that we should first complete normal ordering of a_1 and a_1^\dagger , to include the non-trivial

commutation relation of a_1 and thus the quantum fluctuation of the a_1 mode. This however involves highly complicated calculation.

A huge simplification (and hence a neat explanation of the nature of the quantum noise in the interferometer) however can be made when $\varphi \ll 1$ and $\langle n_{a_2} \rangle \ll 1 \ll |\alpha|^2 \varphi^2$. The fluctuation of the first term in (22) is $\sim \varphi^2 |\alpha|$ (following (19)), whose order of φ is higher than that of the fluctuation of the third term in (24), and therefore is ignored, although the $\sin^2 \langle \varphi a_1^\dagger a_1 \rangle$ term is the main contribution to $\langle n_{b_2} \rangle$ and (18) is still correct, because the expectations of the second and third terms are even smaller. The fluctuation of the second term in (22) is also neglected, because

$$\Delta(a_2^\dagger a_2)^2 = \langle (a_2^\dagger a_2)^2 \rangle - \langle a_2^\dagger a_2 \rangle^2 = \langle a_2^\dagger a_2^\dagger a_2 a_2 \rangle + \langle a_2^\dagger a_2 \rangle - \langle a_2^\dagger a_2 \rangle^2 \simeq 0, \quad (23)$$

compared with the absolute magnitude of $\Delta(a_1^\dagger a_1) = |\alpha|$. Under the above two conditions, approximately we have

$$\Delta n_{b_2} = \sin \varphi \cos \varphi \Delta(a_1^\dagger a_2 - a_2^\dagger a_1). \quad (24)$$

Since the input on the a_1 mode is much stronger than the input on the a_2 mode, it is expected that the a_1 mode looks more classical and the quantum noise comes mainly from the a_2 mode, which we can verify: we have

$$(a_1^\dagger a_2 - a_2^\dagger a_1) = a_1^\dagger a_2 a_1^\dagger a_2 + a_2^\dagger a_1 a_2^\dagger a_1 - \underbrace{a_2^\dagger a_1 a_1^\dagger a_2}_{a_2^\dagger a_2 a_1^\dagger a_1 + a_2^\dagger a_2} - \underbrace{a_1^\dagger a_2 a_2^\dagger a_1}_{a_1^\dagger a_1 a_2^\dagger a_2 + a_1^\dagger a_1},$$

where the last two terms need normal ordering and therefore introduce quantum noise, but the fourth term, which arises because of the commutation relation of a_2 , is much larger than the third term, because $\langle a_1^\dagger a_1 \rangle \gg \langle a_2^\dagger a_2 \rangle$, and therefore we can treat a_1 classically. Therefore we find the final expression of Δn_{b_2} : it is

$$\Delta n_{b_2} = \sin \varphi \cos \varphi \Delta(\alpha^* a_2 - \alpha a_2^\dagger) \approx \varphi \Delta(\alpha^* a_2 - \alpha a_2^\dagger). \quad (25)$$

We can do a sanity check: if the a_2 state is vacuum, then $\langle a_2 \rangle = \langle a_2^\dagger \rangle = 0$, and again due to the non-trivial commutation relation, we have

$$\begin{aligned} \Delta n_{b_2} &\approx \varphi \Delta(\alpha^* a_2 - \alpha a_2^\dagger) = \varphi \sqrt{|\langle (\alpha^* a_2 - \alpha a_2^\dagger)^2 \rangle - \langle (\alpha^* a_2 - \alpha a_2^\dagger) \rangle^2|} \\ &= \varphi \sqrt{|\alpha|^2 \langle a_2 a_2^\dagger \rangle} = \varphi |\alpha| \sqrt{1 + \langle a_2^\dagger a_2 \rangle} = \varphi |\alpha|, \end{aligned} \quad (26)$$

which is the small-angle approximation of (19).

Note that (25) can also be written as

$$\begin{aligned} \Delta n_{b_2} &= \varphi |\alpha| \Delta(e^{-i\phi} a_2 - e^{i\phi} a_2^\dagger) \\ &= \varphi |\alpha| \Delta(-2i \sin \phi \operatorname{Re} a_2 + 2i \cos \phi \operatorname{Im} a_2) \\ &= 2\varphi |\alpha| \Delta(-\sin \phi \operatorname{Re} a_2 + \cos \phi \operatorname{Im} a_2), \end{aligned} \quad (27)$$

where ϕ is the phase of α . The third line has a direct graphic meaning: it has the form of (11) and is proportion to the projection of the “light spot” in $W(\beta, \beta^*)$ on the axis (Fig. 3)

$$\cos \phi \operatorname{Re} \beta + \sin \phi \operatorname{Im} \beta = 0. \quad (28)$$

Thus the quantum noise can be reduced by squeezing the variance on this axis, while still keeping $\varphi \ll 1$ and $|\alpha|^2 \gg \langle n_{a_2} \rangle$.

5 Squeezing the quantum noise

If we inject a squeezed state with parameter $re^{i\theta}$ into the dark port, and let it has narrowest variation in the axis defined by (28), then we have

$$\frac{\theta}{2} - \phi = \frac{\pi}{2}. \quad (29)$$

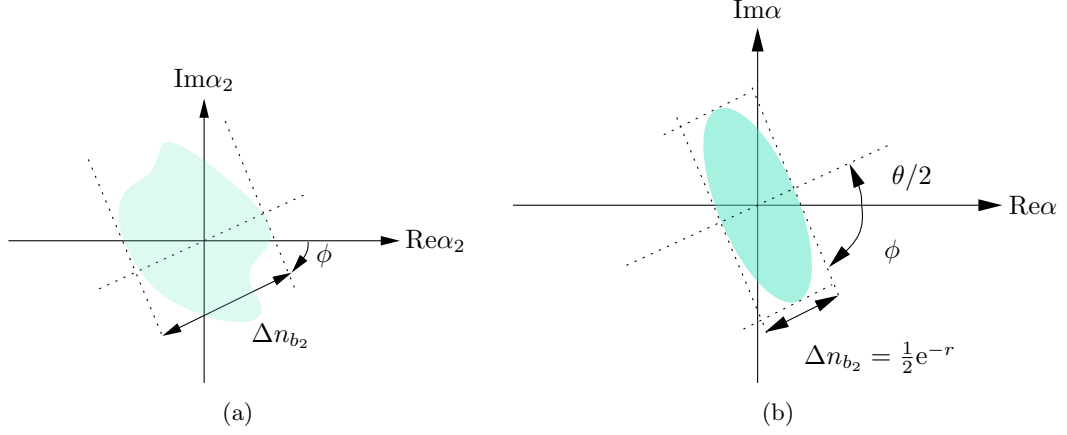


Figure 3: Illustration of (27) in the Wigner phase space of a_2 mode. (a) The variance of n_{b_2} is the distance between two $-\sin \phi \operatorname{Re} a_2 + \cos \phi \operatorname{Im} a_2 = C$ lines, or in other words the projection of the “light spot” on (28). (b) The Wigner function of a squeezed vacuum state injected into the dark port to reduce quantum noise in the output.

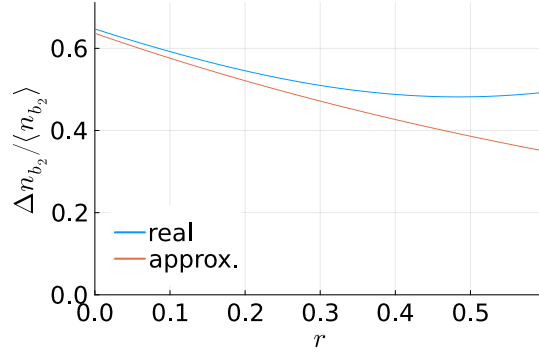


Figure 4: Example of squeezed quantum noise: at $r = 0$ we have the standard quantum limit. Figure plotted using `QuantumOptics.jl` [2]. In the “real” plot, we calculate Δn_{b_2} strictly by definition, i.e. on the tensor product of the a_1 subspace and the a_2 subspace. The photon number cutoff for both spaces is 50, and α is set to 5. The “approx.” plot is drawn according to (30).

This means if we increase r , the relative error seen in n_{b_2} changes as (note that $\langle n_{b_2} \rangle$ is still (18), and we have (27))

$$\frac{\Delta n_{b_2}}{\langle n_{b_2} \rangle} \approx \frac{2|\alpha|\varphi \cdot e^{-r}/2}{|\alpha|^2 \varphi^2} = \frac{1}{|\alpha|\varphi} e^{-r}. \quad (30)$$

Despite the exponent function factor, injecting a squeezed state into the dark port however does not improve the precision of Mach-Zehnder interferometer endlessly: when ξ is very large, the particle number expectation of the a_2 mode is no longer ignorable, breaking one of the two conditions used to derive (25). This is illustrated in Fig. 4, where $\alpha = 2$, $\varphi = \pi/10$, and (29) is followed. The initial difference between two plots arises because of the difference between φ and $\sin \varphi$; it can be seen that as r exceeds 0.3, the shapes of the two curves becomes different, and in reality, increasing r further actually increases the noise of n_{b_2} . Full treatments of the output noise when the dark port receives a squeezed vacuum can be found in [8, 9] and references therein.

6 Conclusion and discussion

Unlike thermal noises arising from escape of information to the reservoir, quantum noise comes from the uncertain nature of physical quantities when we are dealing with a quantum state.

Despite its root in the basic laws of quantum mechanics, quantum noises can be reduced by preparing appropriate initial states, and a toy example is presented above in this report.

The protocol to squeeze quantum noises has already been demonstrated experimentally [10], and the breakdown of the squeezing scheme with strong squeezing outlined above can be avoided by extracting information from the fluctuation pattern of the output signal [9], or with the so-called $N00N$ state [11]. However, these protocols are bound by a $1/N$ ($\simeq 1/|\alpha|^2$) quantum limit: the Heisenberg limit, which roughly corresponds to the particle number-phase uncertainty principle: what we measure is in essence a phase difference between two beams of light, and then $\Delta\theta \sim 1/\Delta N \sim 1/N$, though a more rigid proof is required [12]. Despite often being depicted as the ultimate quantum limit, by so-called nonlinear measurement, measurements beyond the Heisenberg limit are possible [13, 14].

A final remark on quantum noise squeezing is that the above discussions are no longer illusory, because the precisions of the most advanced gravitational wave detectors have already entered the region where quantum noises are important. The squeezed state injection protocol has already been implemented on GEO 600 and LIGO [7, 15] and resulted in expected reduction of noises.

References

- [1] Robert Zwanzig. *Nonequilibrium statistical mechanics*. Oxford university press, 2001. The discussion on Mori-Zwanzig formalism or “generalized Langevin equation” can be found on page 149.
- [2] Sebastian Krämer et al. “QuantumOptics.jl: A Julia framework for simulating open quantum systems”. In: *Computer Physics Communications* 227 (2018), pp. 109–116.
- [3] Marlan O Scully and M Suhail Zubairy. *Quantum Optics*. American Association of Physics Teachers, 1999. Eq. (2.7.3) defines the squeezing operator. Eqs. (2.7.8) and (2.7.9) are about quantum noise in a squeezed state. Eq. (3.3.14) is the definition of Wigner function.
- [4] Daniel A Steck. *Quantum and atom optics*. 2007. URL: <http://atomoptics.uoregon.edu/~dsteck/teaching/quantum-optics/quantum-optics-notes.pdf>. See p. 406 for discussion on quantization of electromagnetic field.
- [5] Carlton M Caves. “Quantum-mechanical noise in an interferometer”. In: *Physical Review D* 23.8 (1981), p. 1693.
- [6] Carlton M Caves. “Quantum-mechanical radiation-pressure fluctuations in an interferometer”. In: *Physical Review Letters* 45.2 (1980), p. 75.
- [7] “A gravitational wave observatory operating beyond the quantum shot-noise limit”. In: *Nature Physics* 7.12 (2011), pp. 962–965.
- [8] D.F. Walls and G.J. Milburn. *Quantum Optics*. Springer Berlin Heidelberg, 2008. See p. 173 for discussion on squeezing quantum noises. Note that the scattering matrix (and therefore the detection scheme) used in this book is different from this report.
- [9] Luca Pezzé and Augusto Smerzi. “Mach-Zehnder interferometry at the Heisenberg limit with coherent and squeezed-vacuum light”. In: *Physical Review Letters* 100.7 (2008), p. 073601.
- [10] Min Xiao, Ling-An Wu, and H Jeffrey Kimble. “Precision measurement beyond the shot-noise limit”. In: *Physical Review Letters* 59.3 (1987), p. 278.
- [11] Vittorio Giovannetti, Seth Lloyd, and Lorenzo Maccone. “Advances in quantum metrology”. In: *Nature Photonics* 5.4 (2011), pp. 222–229. ISSN: 1749-4893.
- [12] Vittorio Giovannetti, Seth Lloyd, and Lorenzo Maccone. “Quantum metrology”. In: *Physical Review Letters* 96.1 (2006), p. 010401.
- [13] Sergio Boixo et al. “Quantum metrology: dynamics versus entanglement”. In: *Physical Review Letters* 101.4 (2008), p. 040403.
- [14] M. Napolitano et al. “Interaction-based quantum metrology showing scaling beyond the Heisenberg limit”. In: *Nature* 471.7339 (2011), pp. 486–489.

- [15] J. Aasi et al. “Enhanced sensitivity of the LIGO gravitational wave detector by using squeezed states of light”. In: *Nature Photonics* 7.8 (2013), pp. 613–619.